A Chromosomal Inversion within a Quantitative Trait Locus Has a Major Effect on Adipogenesis and Osteoblastogenesis

CHERYL L. ACKERT-BICKNELL,[a] JESSE L. SALISBURY,[a,b]
MARK HOROWITZ,[c] VICTORIA E. DeMAMBRO,[a]
LINDSAY G. HORTON,[a] KATHRYN L. SHULTZ,[a]
BEATA LECKA-CZERNIK,[d] AND CLIFFORD J. ROSEN[a]

[a] The Jackson Laboratory, Bar Harbor, Maine, USA

[b] Graduate School for Biomedical Science, University of Maine, Orono, Maine, USA

[c] Yale University School of Medicine, New Haven, Connecticut, USA

[d] University of Arkansas Medical Center, Little Rock, Arkansas, USA

ABSTRACT: We mapped a quantitative trait locus (QTL) for BMD to mid-distal chromosome (Chr) 6 in a cross between C57BL/6J (B6) and C3H/HeJ (C3H). The B6.C3H-6T (6T) congenic was developed to map candidate genes in this QTL. Recently, a 25 cM paracentric inversion was discovered on Chr 6 in C3H/HeJ; we found 6T also carries this inversion. Microarrays from the liver of B6 and 6T uncovered two narrow bands of decreased gene expression in close proximity to the predicted locations of the inversion breakpoints. Changes in specific gene expression in 6T were consistent with its phenotype of low trabecular bone volume and marrow adipogenesis. The BXH recombinant inbred (RI) strains do not carry the C3H/HeJ inversion. To test if the inversion, or allelic effects, were responsible for the 6T phenotype, we made a new congenic, B.H-6, developed by introgressing a 30 Mb region of C3H genomic sequence from BXH6 onto a B6 background. While genetically identical to 6T, this new congenic had a distinct metabolic and skeletal phenotype, with more body fat and greater trabecular BV/TV compared to B6 or 6T. We conclude that the phenotype of 6T cannot be explained by simple allelic differences in one or more genes from C3H. Rather, 6T demonstrates that disordered regulation of gene expression by genomic rearrangement can have a profound effect on a complex trait, such as BMD, and that genomic rearrangement can supersede the effects of various alleles.

Address for correspondence: Dr. Clifford J. Rosen, The Jackson Laboratory, 600 Main Street, Bar Harbor, ME, USA, 04609. Voice: 207-288-6787; fax: 207-288-6073.
rofe@aol.com

INTRODUCTION

Osteoporosis is a disorder associated with increased skeletal fragility.[1,2] Low bone mineral density (BMD), a characteristic feature of this disease, represents the most important risk factor for development of osteoporotic fractures. BMD is a polygenic trait with estimates of heritability ranging up to 80%.[3,4] Polymorphisms in numerous genes, including the Vitamin D receptor (*VDR*), collagen-type 1 (*COL1A1*), estrogen receptor *(ER)*, parathyroid hormone (*PTH*), and insulin-like growth factor 1 (*IGF1*) have been associated with BMD in humans, although each account for a small percentage of the variance in this trait.[5–7] Despite extensive studies with large population cohorts, we are only beginning to understand how genes responsible for the heritable component of this syndrome contribute to fracture risk.[4] Not surprisingly, the mouse has become critical in understanding this process and for hypothesis testing. We identified a quantitative trait locus **(**QTL) for the phenotype of total femoral volumetric BMD and serum IGF-1 on mid-distal Chromosome (Chr) 6 of the mouse, in a cross between the C3H/HeJ (C3H) and C57BL/6J (B6) inbred mouse strains.[8,9] The B6.C3H-6T (6T) congenic strain of mice was developed for the purpose of gaining insight into the biology underlying this QTL and was made by introgressing a region of Chr 6 from C3H onto a B6 background by 10 generations of selective backcrossing. This was followed by several generations of intercrossing to generate mice that were homozygous for B6 alleles for the entire genome, except for the region between *D6Mit93* and *D6Mit216*, which was homozygous for the C3H alleles.[10] Female 6T mice have lower vBMD than either the B6 background strain, or the C3H donor strain mice, and have a smaller periosteal circumference, slightly shorter femurs, and low serum IGF-1. 6T mice also exhibit a decrease in trabecular bone volume fraction (Bone Volume/Total Volume, BV/TV%) of the distal femur that is coincident with an increase in marrow adipocytes and an impairment in osteoblast differentiation.[10,11]

During the development of the B6.C3H-6T congenic strain, we observed that no recombination events occurred between *D6Mit124* and *D6Mit150*. These markers had been mapped in other strains to be greater than 20 cM apart; subsequently we found these two markers to be located more than 45 Mb apart on Chr 6 (http://www.informatics.jax.org/). Further experimentation determined there was a 25 cM paracentric inversion on mid-distal Chr 6 in the C3H/HeJ strain and that the Foundation Stocks for this strain, kept at the Jackson Laboratory (Bar Harbor, ME, USA), are homozygous for this inversion. More specifically, it was found that the *D6Mit124* and *D6Mit150* markers were both

located within the inverted region, but that *D6Mit93* was not. To identify candidate genes related to the QTL of interest, we asked whether the inversion per se, or alleles within the QTL, or both, were responsible for the development of a unique skeletal and metabolic phenotype that included a profound change in stromal cell allocation from preosteoblasts into adipocytes.

MATERIALS AND METHODS

Animal

All strains used for the studies reported herein were obtained from our research colonies at The Jackson Laboratory, Bar Harbor, Maine. All mice were produced by pair matings, with progeny weaned at 22–25 days of age and housed in groups of 2–5 of the same sex in polycarbonate cages (324 cm^2) with sterilized White Pine shavings. Colony environmental conditions included 14:10-h light:dark cycles, with free access to acidified water (pH 2.5 with HCl to retard bacterial growth) that contains 0.4 mg/mL of vitamin K (menadione Na bisulfite), and irradiated NIH31 diet containing 6% fat, 19% protein, Ca:P of 1.15:0.85, plus vitamin and mineral fortification (Purina Mills International, Brentwood, MO, USA). All procedures involving mice were reviewed and approved by the Institutional Animal Care and Use Committee of The Jackson Laboratory.

Microarray

Liver was collected from three 8-week-old B6 and three 6T female mice. Mice were fasted for 5 h before tissue collection. Tissue samples were stored in RNA later (Ambion, Austin, TX, USA) following dissection and later homogenized in TRIzol (Invitrogen, Carlsbad, CA, USA). Total RNA was isolated by standard TRIzol methods according to the manufacturer's protocols, and quality was assessed using a 2100 Bioanalyzer instrument and RNA 6000 Nano LabChip assay (Agilent Technologies, Palo Alto, CA, USA). Following reverse transcription with an oligo(dT)-T7 primer (Affymetrix, Santa Clara, CA, USA), double-stranded cDNA was synthesized with the superscript double-stranded cDNA synthesis custom kit (Invitrogen). In an *in vitro* transcription (IVT) reaction with T7 RNA polymerase, the cDNA was linearly amplified and labeled with biotinylated nucleotides (Enzo Diagnostics, Farmingdale, NY, USA). Fifteen micrograms of biotin-labeled and fragmented cRNA was then hybridized onto MOE430v2.0* GeneChip™ arrays (Affymetrix) for 16 h at 45°C. Posthybridization staining and washing were performed according to the manufacturer's protocols using the Fluidics Station 450 instrument (Affymetrix). Finally, the arrays were scanned with a GeneChip™ Scanner 3000

laser confocal slide scanner. The images were quantified using GeneChip[TM] Operating Software(GCOS) v1.2. Probe level data were imported into the R software environment and expression values were summarized using the Robust MultiChip Average (RMA) function in the R/affy package as previously described.[12] Using the R/maanova package, an analysis of variance (ANOVA) model was applied to the data, and F1, F2, F3, and Fs test statistics were constructed along with their permutation *P*-values. False discovery rate was then assessed using the R/q value package to estimate q-values from calculated test statistics.[12] The data discussed in this publication have been deposited in NCBI's Gene Expression Omnibus (GEO, http://www.ncbi.nlm.nih.gov/geo/) and are accessible through GEO Series accession number GSE5959.

Genotyping

Mice were genotyped by preparing genomic DNA from digestion of 1 mm tail tips in 0.5 mL of 50 mM NaOH for 10 min at 95°C, then pH was adjusted to 8.0 with 1M Tris-HCl. Genotyping of individual mouse DNAs was accomplished by polymerized chain reaction (PCR) using oligonucleotide primer pairs (Mit markers, www-genome.wi.mit.edu/cgi-bin/mouse/index) from several sources (Research Genetics, Birmingham, AL, USA; Invitrogen; IDT, Coralville, IA; Qiagen, Valencia, CA, USA). These primer pairs amplify simple dinucleotide repeated sequences of anonymous genomic DNA that are of different sizes and, via gel electrophoresis, can uniquely discriminate between B6 and C3H genomes. Details of standard PCR reaction conditions have been described previously.[13] PCR products from B6, C3H, and F1 hybrids were used as electrophoretic standards in every gel to identify the genotypes of mice (i.e., *b6/b6, b6/c3, c3/c3*). In addition, three single nucleotide polymorphisms (SNPs) were assayed to further determine the ends of the C3H-like congenic region. Assays for SNPs were performed at KBiosciences, Herts, UK (www.KBioscience.co.uk).

Sequencing

Primers for sequencing were designed using the MacVector sequence analysis package (Version 7.1.1, Accelrys Inc). Cycle sequencing of PCR-DNA templates was performed using Applied Biosystems' BigDye Terminator v3.1 cycle sequencing kit. Sequencing reactions were then purified using Agencourt's CleanSEQ magnetic bead purification system. Purified reactions were run on Applied Biosystems 3730xl DNA Analyzer using POP 7 polymer. Raw data files were analyzed using Applied Biosystems DNA Sequencing Analysis Software, Version 5.2.

Development of the B.H-6 Congenic Strain

BHX6 mice were mated with B6 progenitor strain mice and the offspring mated back to B6. Mice were typed at each generation for the markers *D6Mit102*, *D6Mit320*, *D6Mit108*, *D6Mit366*, and *D6Mit150* (Mit markers, www.genome.wi.mit.edu/cgi-bin/mouse/index) and mice that were *c3/b6* for all of these markers were backcrossed to B6. This was repeated until eight generations of backcrossing had been achieved. The N8F1 mice were inter-crossed producing N8F2 progeny. Mice homozygous for the C3H-like alleles were further intercrossed for two more generations, yielding N8F4. This new congenic was named B.H-6.

Body Composition

Areal BMD and body composition were assessed using peripheral dual-energy X-ray absorptiometry (PIXImus, GE-Lunar, Madison, WI, USA). Whole body (exclusive of the head) composition measures of lean mass, fat mass, and a percentage of body fat were obtained.

Necropsy for Femur Collection

All bones for density and architecture analysis were collected from female, 16-week-old mice. This is the age at which mice have acquired their adult femoral mass.[14] Mice were necropsied, whole body weights recorded, and tissue samples collected. Skeletal preparations (lumbar vertebral columns, pelvis, and attached hind limbs) were placed in 95% EtOH for a period of not less than 2 weeks. Femurs were dissected free of remaining muscle and connective tissue, and placed in 95% EtOH for storage until subsequent analyses were conducted.

pQCT for Volumetric (v)BMD Bone Densitometry

Femur lengths were measured with digital calipers (Stoelting, Wood Dale, IL, USA) and then measured for density using the SA Plus densitometer (Ortho-metrics, Stratec SA Plus Research Unit, White Plains, NY, USA). Calibration of the SA Plus instrument was established with hydroxyapatite standards of known density (50–1,000 mg/mm^3) with cylindrical diameters 2.4 mm and length 24 mm that approximate mouse femurs. Daily quality control of the SA Plus instrument's operation was checked with a manufacturer-supplied phantom. The bone scans were analyzed with threshold settings to separate bone from soft tissue. Thresholds of 710 and 570 mg/cm^3 were used to determine

cortical bone areas and surfaces that yielded area values consistent with histomorphometrically derived values. To determine mineral content, a second analysis was carried out with thresholds of 220 and 400 mg/cm^3 selected so that mineral from most partial voxels (0.07 mm) was included in the analysis. Density values were calculated from the summed areas and associated mineral contents. Precision of the SA Plus for repeated measurement of a single femur was found to be 1.2–1.4%. Isolated femurs were scanned at seven locations at 2 mm intervals, beginning 0.8 mm from the distal ends of the epiphyseal condyles. Total vBMD values were calculated by dividing the total mineral content by the total bone volume and expressed as mg/mm^3.

Micro-CT40 for Distal Trabecular Bone

Femurs were scanned using a Micro-CT40 microcomputed tomographic instrument (Scanco Medical AG, Bassersdorf, Switzerland) to evaluate trabecular bone volume fraction and microarchitecture in the secondary spongiosa of the distal femur. Daily quality control of the instrument's operation was checked with a manufacturer-supplied phantom. The femurs were scanned at low-resolution energy level of 55KeV, and intensity of 145 μA. Approximately 100 slices were measured just proximal to the distal growth plate, with an isotropic pixel size of 12 μm and slice thickness of 12 μm. Trabecular bone volume fraction (%BV/TV) and microarchitecture properties were evaluated in the secondary spongiosa, starting ∼ 0.6 mm proximal to the growth plate, and extending proximally 1.5 mm.

Statistical Assessment

Data are expressed as mean ± SEM in tables and figures. Statistical evaluation of bone and body composition was conducted using JMP version 6 software (SAS, Cary, NC, USA). To account for differences in body size between strains, a stepwise ANCOVA approach was used for PIXI, pQCT, and μCT data using body weight and femur length as covariates. Nonsignificant covariates and interactions were removed in a stepwise fashion until the final model was obtained.

RESULTS

Determining the End Points of the Inversion

We previously published that the upper breakpoint of the inversion was proximal to *D6Mit124* (at 71.3 Mb, NCBI Build 36) and the lower breakpoint was distal to *D6Mit150* (at 116.1 Mb, NCBI Build 36).[15] Recombination between
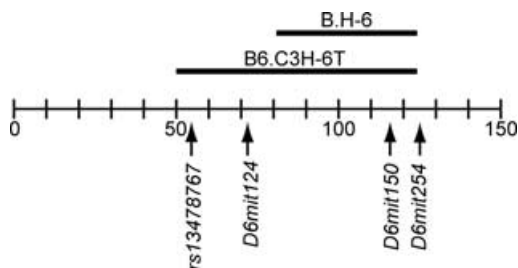
FIGURE 1. Relationship between the 6T and B.H-6 congenics with the inversion breakpoints are shown. Vertical ticks indicate 10 Mb intervals along Chr 6. The upper breakpoint of the inversion is located between *rs13478767 and D6Mit124* and the lower breakpoint is located between *D6Mit150* and *D6Mit254*. The 6T congenic was made by introgressing the region between *D6Mit93* (at 52 Mb, not shown) and *D6Mit150* from C3H on the B6 background by selective backcrossing.[10] Further mapping has shown that the C3H-like region extends to *D6Mit216* (at 121.1 Mb), but not to *Dmit254*. The new B.H-6 congenic carries C3H-like alleles from *D6Mit102* to rs3727110 at 122.0 Mb.

C3H and strains not carrying the inversion is not possible within the inverted region. To further resolve the location of the inversion breakpoints, we examined recombination patterns in the original B6XC3H F2 mapping cross in which the BMD QTL on Chr 6 was discovered. This cross is described in detail elsewhere.[8,9] The markers *D6Mit93* and *D6Mit124* were typed in the original mapping analysis. *D6Mit124* was clearly located within the inverted region, whereas *D6Mit93* was not. We then found that 21 mice in the F2 cross had had a recombination event between these two markers. We typed these mice for the following markers, *D6Mit183*, *D6Mit175*, and *D6Mit17*. In four of the 21 mice, a recombination event that had occurred between *D6Mit183* and *D6Mit175* was found, but there were no recombination events distal to *D6Mit175*. We then sequenced *rs13478767*, a SNP located between *D6Mit183* and *D6Mit175* and found that in one mouse, recombination events distal to *rs13478767* had occurred. We therefore concluded that the upper inversion breakpoint must be distal to *rs13478767,* located at 55.2 Mb (NCBI Build 36), but proximal to *D6Mit124* at 71.3 Mb.

We employed a similar strategy to determine the location of the lower breakpoint. We knew from the FISH analysis that *D6Mit150* was located within the inverted region.[15] The next marker typed in the original F2 mapping cross was *D6Mit59*, located at 138.8 Mb. To narrow the possible interval in which the breakpoint could be located, we then typed *D6Mit254* (at 125.3 Mb), *D6Mit135* (at 128.8 Mb), and *D6Mit219* (132.4 Mb) in DNA from 11 of the original F2 mapping cross mice. We found that a recombination event had occurred between the markers *D6Mit150* and *D6Mit254* in 2 of the 11 mice examined. Therefore, we concluded that the lower inversion breakpoint was distal to *D6Mit150*, but proximal to *D6Mit254*. The locations of these markers, relative to the C3H-like congenic region of the 6T strain, are shown in FIGURE 1.
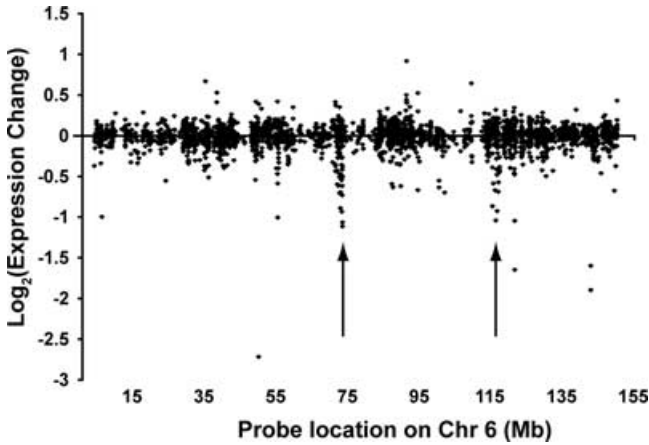
FIGURE 2. Gene expression levels in the liver of female 6T mice, relative to age-matched female B6 mice, was examined by microarray. We plotted the genomic location, in Mb (NCBI Build 36), to which each probe set mapped versus relative expression level. As can be seen here, there is a clear pattern of decreased gene expression at ∼72 Mb and at ∼116 Mb, as indicated by the black arrows. These zones of decreased gene expression are located in close proximity to the predicted breakpoints for the paracentric inversion found in C3H/HeJ. This inversion is carried in the 6T congenic strain.

Gene Expression Along Chromosome 6 in B6.C3H-6T

We next examined the pattern of differential gene expression on Chr 6 in the liver of 6T and B6 by microarray. Relative expression change for each probe set was calculated as described above. We then plotted expression changes in 6T versus the chromosomal location of the probe set. As can be seen in FIGURE 2, there are scattered genes along Chr 6 that show significantly high or low gene expression, as expected. Expression changes in these genes are likely, either directly or indirectly, due to a consequence of allelic differences between these two strains. Interestingly, at approximately 72 Mb and 116 Mb, a clear pattern gene of expression emerges. In other words, in these two locations, that is, the breakpoints of the inversion, the majority of genes are clearly downregulated in 6T liver.

Development of the B.H-6 Congenic Strain

To test the hypothesis that the inversion was responsible for the differential gene expression, we looked to another set of inbred strains. The BXH recombinant inbred (RI) strains were generated from crosses between the B6 and the C3H/HeJ strains.[16] These RI strains were developed in the early 1970s, and must have been made either before the inversion arose on Chr 6
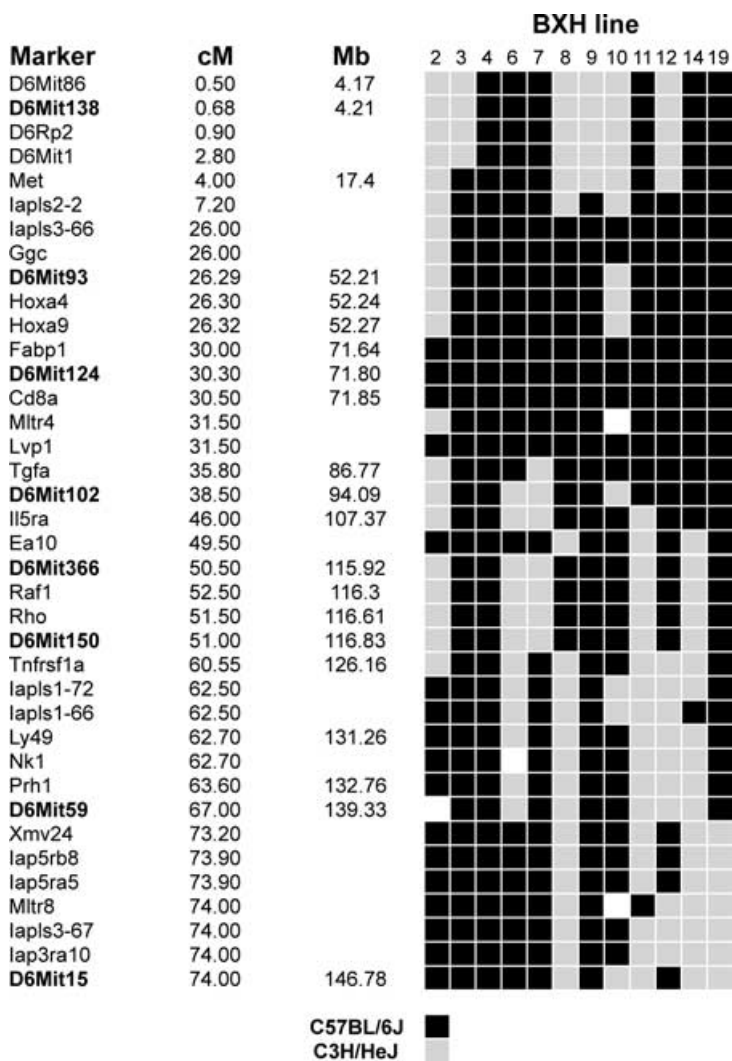
FIGURE 3. Mapping data for 12 of the BXH RI strains were obtained from the mouse genome database. The map location in CentiMorgans (CM) and the genomic region (if available) were also determined for all markers. Eight additional markers (*in bold*) were typed for all 12 lines. C3H-like alleles are shown in gray and B6-like alleles are shown in black. Data were not obtainable for all strains for all markers (denoted by white squares).

in C3H/HeJ or before this inversion became fixed, as none of the resulting BXH RI lines are *c3/c3* for the entire inversion region (FIG. 3). To determine if the low BMD and low serum IGF-1 phenotypes of the 6T congenic mouse were a function of allelic differences from C3H, or due entirely to the Chr

TABLE 1. Anthropomorphic aspects of three strains of mice

	C57BL/6J	B6.C3H-6T	B.H-6
Body weight (g) [a]	20.12 ± 0.34	19.32 ± 0.62	21.44 ± 0.66
Lean mass (g) [b,c]	14.37 ± 0.10	14.76 ± 0.19	13.70 ± 0.20*, **
% Total body fat [b,c,d]	19.60 ± 0.33	15.48 ± 0.91*	22.02 ± 0.87*, **

[a]The covariate strain was not significant.
[b]Strain was a significant covariate.
[c]Body weight was a significant covariate.
[d]Strain X Body weight was a significant covariate.
*Significantly different than C57BL/6J ($p = 0.05$).
**Significantly different than B6.C3H-6T ($p = 0.05$).

6 inversion, we then generated a new congenic strain, B.H-6. The allele distribution patterns of the 12 remaining BXH RI lines are publicly available at (http://www.informatics.jax.org/searches/riset˙form.shtm). We obtained DNA from these 12 strains and further genotyped them for 8 additional markers (*D6Mit138*, *D6Mit93*, *D6mit124*, *D6Mit102*, *D6Mit366*, *D6mit150*, *D6Mit59,* and *D6Mit15*). Two lines carried C3H-like alleles for the majority of the genomic region that is inverted in the present day C3H/HeJ strain: BXH2 and BXH6 (FIG. 3). BXH6 was chosen as the donor strain for the congenic because: (1) we were concerned that the C3H-like region of BXH2 did not extend distal enough, and (2) the proximal end of the region of interest in BXH2 appears to have undergone extensive recombination, resulting in short alternating stretches of B6-like and C3H-like sequences.

The B.H-6 congenic was generated by introgressing an approximately 30 Mb region of Chr 6 from the BXH6 RI line onto a B6 background, by eight generations of backcrossing. The B.H-6 congenic mice are *c3/c3* for the region between *D6Mit102* and *D6Mit150*, but are otherwise *b6/b6* for the remainder of the genome. Additional SNP testing was done on the N8F4 generation mice to further determine the ends of the C3H-like congenic region. It was determined that the B.H-6 congenic is *b6/b6* like at *rs3708822* at 89.3 Mb (NCBI build 36) but is *c3/c3* like at *D6Mit102* at 93.4 Mb (NCBI build 36). At the distal end the B.H-6 congenic is *c3/c3* as far distal as *rs3727110* at 122.0 Mb (NCBI build 36).

Phenotype of the B.H-6 Congenic

At 16 weeks of age, female B.H-6 congenic weigh more than both the B6 progenitor and the 6T congenic stain, although the covariate of strain was not significant in the ANCOVA fit model. Female B.H-6 mice had higher absolute fat mass (data not shown), and a higher percentage of total body fat than either B6 or 6T. In addition, this strain had a lower lean mass, as noted in TABLE 1. Unlike the 6T congenic, 16-week-B.H-6 female mice had similar total femoral

TABLE 2. Differences in the cortical bone mass for three strains of mice

	C57BL/6J	B6.C3H-6T	B.H-6
Total vBMD (mg/mm^3) [a,b,d]	0.585 ± 0.004	0.530 ± 0.006*	0.587 ± 0.007**
Total cortical vBMD (mg/mm^3) [a,b]	1.099 ± 0.002	1.085 ± 0.003*	1.086 ± 0.003*
Cortical thickness (mm)[a,b]	0.190 ± 0.001	0.174 ± 0.001*	0.181 ± 0.002*,**
Periosteal circumference (mm) [a,b,c]	4.88 ± 0.02	4.77 ± 0.02*	4.89 ± 0.02**
Endosteal circumference (mm) [a,c]	3.68 ± 0.02	3.67 ± 0.01	3.76 ± 0.02*,**

[a] Strain was a significant covariate.
[b] Femur length was a significant covariate.
[c] Body weight was a significant covariate.
[d] Strain X Femur length was a significant covariate.
*Significantly different than C57BL/6J ($p = 0.05$).
**Significantly different than B6.C3H-6T ($p = 0.05$).

TABLE 3. Differences in the distal trabecular region of the femur in three strains

	C57BL/6J	B6.C3H-6T	B.H-6
BV/TV (%) [a]	8.17 ± 0.3	6.02 ± 0.4*	9.46 ± 0.4*,**
Trabecular number (/mm) [a,b,c,d,e]	3.80 ± 0.05	3.53 ± 0.06*	4.04 ± 0.05*,**
Trabecular thickness (μm)[f]	0.0471 ± 0.0007	0.0465 ± 0.001	0.0493 ± 0.0009
Connectivity density (mm^{-3}) [a]	61.86 ± 3.21	34.69 ± 4.53*	70.96 ± 3.98**
SMI [a]	2.90 ± 0.04	3.27 ± 0.04*	2.81 ± 0.05**

[a] Strain was a significant covariate.
[b] Body weight was a significant covariate.
[c] Femur length was a significant covariate.
[d] Femur length X Body weight was a significant covariate.
[e] Strain X Femur length was a significant covariate.
[f] The covariate strain was not significant.
*Significantly different than C57BL/6J ($p = 0.05$).
**Significantly different than B6.C3H-6T ($p = 0.05$).

volumetric BMD (vBMD) compared to the B6 progenitor strain. Interestingly, like 6T, B.H-6 mice had reduced cortical vBMD and had thinner cortices at the midshaft of the femur than B6 (TABLE 2). While there was no difference between B6 and B.H-6 for periosteal circumference, the endosteal circumference at the midshaft of the femur was larger in B.H-6 (TABLE 2). Most impressively, the B.H-6 mice had a striking increase in BV/TV% of the distal femur, compared to either the B6 or the 6T strains. This increase in trabecular bone volume was primarily a function of more trabeculae, rather than a significant change in trabecular thickness (TABLE 3). The structure model index (SMI) of the distal femoral trabecular bone was lower in B.H-6, indicating a more plate-like appearance to the trabeculae, as can be seen in FIGURE 4.

FIGURE 4. Trabecular bone architecture was examined in the distal femur of female, 16-week-old C57BL/6J (B6), B6.C3H-6T (6T), and B.H-6 mice. The BV/TV% was greatly increased in the B.H-6 strain, compared to either the B6 progenitor strain, or the 6T congenic, which carried the inversion from C3H/HeJ. In addition, the trabecular number was greatly increased in B.H-6. There was an increase in trabecular thickness, but this was not statistically significant.

DISCUSSION

The arrangement of genes within the eukaryotic genome is not random. Studies have shown that functionally related genes can be found clustered within discrete blocks. These blocks can be as large as several megabases in mammals (reviewed in Hurst *et al*.[17]). One such block exists in mice at the distal end of the 6T congenic region. Between 115 and 125 Mb, several genes involved in adipocyte maturation and fatty acid metabolism, as well as osteoblast differentiation, can be found, including *Pparg*, *Alox5*, *Adipor2,* and *Tpi1*. Disruption in the organization and order of genes within the genome, without disturbing the structure of a gene unit, can cause a variety of human diseases.[18] In this article we show that the 6T and B.H-6 congenic strains, despite having the same *C3H* alleles on distal Chr 6 and identical B6 backgrounds, have a drastically different anthropomorphic and skeletal phenotype; that is, 6T is a small lean mouse with very low BMD but marrow adipogenesis, whereas B.H-6 is fatter with higher BMD. These data support the thesis that the chromosomal inversion, not the allelic differences between C3H and B6, is responsible for the metabolic and skeletal phenotypes of 6T.

The most likely candidate gene to be disrupted by this inversion because of its genomic location is *Pparg*, a nuclear receptor that is essential for adipogenesis, and also a negative regulator of osteoblastogenesis when activated by specific ligands. We previously showed that *Pparg* expression is increased in calvarial osteoblasts from 6T, compared to B6, although in the liver, *Pparg* expression was significantly downregulated in 6T versus B6.[11] To determine if *Pparg* was involved in the 6T phenotype, we recently identified two SNPs in the promoter region of exon B, adjacent to a Cebpa-binding site, which codes for

TABLE 4. Assessment of the effects of allelic differences found within the C3H/HeJ *Pparg2* promoter on promoter function. (WT — B6-like, Mut — C3H-like, $^*p < 0.001$)

Treatment	48 h	% Decrease	72 h	% Decrease
WT	16.64 ± 0.58		28.40 ± 1.63	
Mut	11.1 ± 0.48	-32^*	16.5 ± 0.6	-42^*
WT + CEBPα	47.07 ± 8.31		54.4 ± 0.96	
Mut + CEBPα	36.0 ± 1.1	-23^*	39.0 ± 4.5	-26^*
No transfection	0.18 ± 0.04		0.45 ± 0.06	
CEBPα alone	0.02 ± 0.01		0.04 ± 0	

The B6 (WT) *Pparg2* promoter was cloned into a pGL3 Luciferase expression vector (Promega, Madison, WI). Two polymorphisms from the C3H/HeJ strain were introduced using the QuikChange Site Directed Mutagenesis kit (Stratagene, La Lolla, CA) and this construct was referred to as "Mut." Constructs were transfected into UAMS33 cells and cells were treated with either vehicle or vehicle + CEBPA. Luciferase expression is presented at 48 and 72 h. Transfection efficiency was controlled by co-transfection with a Renilla expression vector (pRL-SV40, Promega, Madison, WI).

expression of the PPARG2 protein that is fat specific. Transient transfection of this promoter polymorphism containing a C3H sequence into UAMS stromal cells resulted in significant downregulation of *Pparg* expression, consistent with a hypomorphic polymorphism in the parental C3H mouse (see TABLE 4). Interestingly, homozygous *Pparg*$^{-/-}$ mice (*Pparg*^{tm1Tka}) die at embryonic day 10.5 to 11 *post coitum* due to placental insufficiency but the *Pparg*$^{+/-}$ mouse is viable and appears to have normal development of all major organs.[19] *Pparg*$^{+/-}$ mice have higher areal BMD by DXA and markedly increased trabecular bone volume (BV/TV%) at 8 weeks of age compared to wildtype.[20] Moreover, it appears these mice maintain a higher BV/TV% than controls through 52 weeks of age, suggesting resistance to age-related trabecular bone loss.[20] The increase in bone volume fraction is strikingly similar to the skeletal phenotype of the B.H-6 congenic strain and most likely represents a significant genetic contribution from C3H (i.e., a hypomorphic polymorphism), which also has increased bone volume fraction in the distal femur. On the other hand, 6T mice have reduced bone volume fraction, despite the allelic effects of the C3H polymorphism, strongly suggesting that the inversion has disrupted the regulation of this gene, resulting in marrow adipogenesis, impaired osteoblast differentiation, and low bone mass.

In conclusion, we have created two mouse strains with nearly identical alleles for genes in the distal region of Chr 6, but with widely different metabolic and skeletal phenotypes. The chromosomal inversion in distal Chr 6 clearly determines the effects of several closely related genes on fat and bone. Further studies of the regulatory region 3′ to the inversion breakpoint will help determine the evolutionary significance of this genomic region and provide us with a better understanding of the relationship between adipogenesis and osteoblastogenesis.

ACKNOWLEDGMENT

REFERENCES

1. COMPSTON, J. & C.J. ROSEN. 2006. *Fast Facts: Osteoporosis*. Fifth edition. Health Press. Oxford.
2. 1994. WHO assessment of fracture risk and its application to screening for post-menopausal osteoporosis. WHO technical reports series **834:**
3. CUSACK, S. & K. CASHMAN. 2003. Impact of genetic variation on metabolic response of bone to diet. Proc. Nutr. Soc. **62:** 901–912.
4. RALSTON, S. & B. DE CROMBRUGGHE. 2006. Genetic regulation of bone mass and susceptibility to osteoporosis. Genes Dev. **20:** 2492–2506.
5. THAKKINSTIAN, A., C. D'ESTE, J. EISMAN, *et al*. 2004. Meta-analysis of molecular association studies: vitamin D receptor gene polymorphisms and BMD as a case study. J. Bone Miner. Res. **19:** 419–428.
6. BUSTAMANTE, M., X. NOGUES, A. ENJUANES, *et al*. 2007. COL1A1, ESR1, VDR and TGFB1 polymorphisms and haplotypes in relation to BMD in Spanish post-menopausal woman. Osteoporos. Int. **18:** 235–243.
7. RIVADENEIRA, F., J. HOUWING-DUISTERMAAT, N. VAESSEN, *et al*. 2003. Association between an insulin-like growth factor 1 gene promoter polymorphism and bone mineral density in the elderly: the Rotterdam Study. J. Clin. Endocrinol. Metab. **88:** 3878–3884.
8. BEAMER, W.G., K.L. SHULTZ, L.R. DONAHUE, *et al*. 2001. Quantitative trait loci for femoral and lumbar vertebral bone mineral density in C57BL/6J and C3H/HeJ inbred strains of mice. J. Bone Miner. Res. **16:** 1195–1206.
9. ROSEN, C.J., G. CHURCHILL, L.R. DONAHUE, *et al*. 2000. Mapping quantitative trait loci for serum insulin-like growth factor-I levels in mice. Bone **27:** 521–528.
10. BOUXSEIN, M.L., C.J. ROSEN, C.H. TURNER, *et al*. 2002. Generation of a new congenic mouse strain to test the relationship among serum insulin-like growth factor I, bone mineral density and skeletal morphology *in vivo*. J. Bone Miner. Res. **17:** 570–579.
11. ROSEN, C.J., C. ACKERT-BICKNELL, M.L. ADAMO, *et al*. 2004. Congenic mice with low serum IGF-1 have increased body fat, reduced bone mineral density, and an altered osteoblast differentiation program. Bone **35:** 1046–1058.
12. SHOCKLEY, K. & G.A. CHURCHILL. 2006. Gene expression analysis of mouse chromosome substitution strains. Mammalian Genome **17:** 598–614.
13. SVENSON, K., Y.-C. CHEAH, K.L. SHULTZ, *et al*. 1995. Strain distribution pattern for the SSLP markers in the SWXJ recombinant inbred strain set: chromosomes 1 to 6. Mammalian Genome **6:** 867–872.
14. BEAMER, W.G., L.R. DONAHUE, C.J. ROSEN, *et al*. 1996. Genetic variability in adult bone density among inbred strains of mice. Bone **18:** 397–403.
15. AKESON, E.C., L.R. DONAHUE, W.G. BEAMER, *et al*. 2006. Chromosomal inversion discovered in C3H/HeJ mice. Genomics **87:** 311–313.

16. TAYLOR, B.A., H.G. BEDIGIAN & H. MEIER. 1977. Genetic studies of the Fv-1 locus in mice: linkage with Gpd-1 in recombinant inbred lines. J. Virol. **23:** 106–109.

17. HURST, L., C. PAL & M. LERCHER. 2004. The evolutionary dynamics of eukaryotic gene order. Nat. Rev. Genet. **5:** 299–310.

18. KLEINJAN, D. & V. VAN HEYNINGEN. 2005. Long-range control of gene expression: emerging mechanisms and disruption in disease. Am. J. Hum. Genet. **76:** 8–32.

19. BARAK, Y., M.C. NELSON, E.S. ONG, *et al*. 1999. PPAR gamma is required for placental, cardiac, and adipose tissue development. Mol. Cell **4:** 585–595.

20. AKUNE, T., S. OHBA, S. KAMEKURA, *et al*. 2004. PPARgamma insufficiency enhances osteogenesis through osteoblast formation from bone marrow progenitors. J. Clin. Invest. **113:** 846–855.